



Calculated densities of $\text{H}_3\text{O}^+(\text{H}_2\text{O})_n$, $\text{NO}_2^-(\text{H}_2\text{O})_n$, $\text{CO}_3^-(\text{H}_2\text{O})_n$ and electron in the nighttime ionosphere of Mars: Impact of solar wind electron and galactic cosmic rays

S. A. Haider,¹ V. Singh,² V. R. Choksi,¹ W. C. Maguire,³ and M. I. Verigin⁴

Received 9 May 2007; revised 13 August 2007; accepted 4 October 2007; published 29 December 2007.

[1] We have calculated the densities of positive ions and negative ions in the ionosphere of Mars at solar zenith angle 106° between height interval 0 km and 220 km.

This model couples ion-neutral, electron neutral, dissociation of positive and negative ions, electron detachment, ion-ion, ion-electron recombination processes through 117 chemical reactions. Of the 34 ions considered in the model, the chemistry of 17 major ions (O_2^+ , NO^+ , CO_2^+ , $\text{H}_3\text{O}^+\text{H}_2\text{O}$, $\text{H}_3\text{O}^+(\text{H}_2\text{O})_2$, $\text{H}_3\text{O}^+(\text{H}_2\text{O})_3$, $\text{H}_3\text{O}^+(\text{H}_2\text{O})_4$, O_2^+CO_2 , H_3O^+ , CO_4^- , CO_3^- , $\text{CO}_3^-\text{H}_2\text{O}$, $\text{CO}_3^-(\text{H}_2\text{O})_2$, $\text{NO}_2^-\text{H}_2\text{O}$, $\text{NO}_2^-(\text{H}_2\text{O})_2$, $\text{NO}_3^-\text{H}_2\text{O}$, and $\text{NO}_3^-(\text{H}_2\text{O})_2$) are discussed in this paper. At altitude below 70 km, the electron density is mainly controlled by hydrated hydronium ions and water clusters of NO_2^- and CO_3^- .

The ions O_2^+ and NO^+ dominate above this altitude. This calculation suggests that the ionosphere of Mars contains *F* and *D* peaks at altitude ~ 130 km and ~ 30 km due to precipitation of solar wind electron and galactic cosmic rays respectively. *F* peak is mainly produced by O_2^+ after heavy loss of CO_2^+ with atomic oxygen. *D* peak occurs due to high efficiency of electron attachment to *Ox* molecules, which entails that concentration of negative ions is higher than that of electron below 30 km. These results are compared with radio measurements made by Mars 4 and Mars 5 in the nighttime ionosphere.

Citation: Haider, S. A., V. Singh, V. R. Choksi, W. C. Maguire, and M. I. Verigin (2007), Calculated densities of $\text{H}_3\text{O}^+(\text{H}_2\text{O})_n$, $\text{NO}_2^-(\text{H}_2\text{O})_n$, $\text{CO}_3^-(\text{H}_2\text{O})_n$ and electron in the nighttime ionosphere of Mars: Impact of solar wind electron and galactic cosmic rays, *J. Geophys. Res.*, 112, A12309, doi:10.1029/2007JA012530.

1. Introduction

[2] The ionosphere of Mars has been observed by radio occultation experiment during the encounters of Mariner 4 [Kliore *et al.*, 1965], Mariner 6, 7 [Fjeldbo *et al.*, 1970], Mars 2 [Kolosov *et al.*, 1976], Mariner 9 [Kliore *et al.*, 1972], Mars 4, 5 and 6 [Vasiliev *et al.*, 1975], Viking 1/2 [Fjeldbo *et al.*, 1977] and Mars Global Surveyor [Hinson *et al.*, 1999]. Unfortunately only five electron density profiles are available in the night side ionosphere of Mars from these observations. Among them two profiles were observed at latitude $\sim 37^\circ$ – 38°N from Mars 4 and Mars 5 above the Martian surface on 10 and 18 February 1974 respectively at solar zenith angle $\sim 106^\circ$ [Savich and Samovol, 1976]. These observations represent that nighttime ionosphere of Mars contains three peaks at altitude range ~ 30 – 35 km, ~ 110 – 130 km and ~ 180 – 200 km, which are produced by different physical processes. However, other data obtained from these measurements suggest that sometimes these

peaks were not visible. There have been no measurements for ion compositions in the lower ionosphere of Mars.

[3] Recently, Seth *et al.* [2002] and Haider *et al.* [2002] have reported that Martian magnetic field near the terminator changes its direction from horizontal to vertical, which allows for ionospheric loss above 100 km due to solar wind electron precipitation in the night hemisphere. Molina-Cuberos *et al.* [2002] have calculated nighttime electron density below 100 km due to precipitation of galactic cosmic rays. These papers have generated new interest on this topic. In the present paper, we have used these two sources of ionization in ion-neutral model to calculate the concentrations of positive ions, negative ions and electron in the nighttime Martian ionosphere between altitude 0 km and 220 km. This model couples ion-neutral, electron neutral, dissociation of positive and negative ions, electron detachment, ion-ion, ion-electron recombination process through 117 chemical reactions. It is found that the nighttime ionosphere of Mars can be divided into *D* and *F* regions by analogy to Earth's ionosphere. The *D* peak is formed at altitude ~ 30 km with the electron concentration 100 cm^{-3} due to absorption of galactic cosmic rays in the energy range 1–1000 GeV. The *F* peak is formed at altitude range ~ 125 – 135 km with the total ion concentration $5.2 \times 10^3\text{ cm}^{-3}$ due to precipitation of solar wind electron in the energy range 1–1000 eV. In the chemistry of positive ions,

¹Physical Research Laboratory, Ahmedabad, India.

²Universita' degli Studi di Brescia, Italy.

³NASA Goddard Space Flight Centre, Greenbelt, Maryland, USA.

⁴Space Research Institute, Moscow, Russia.

hydrated hydronium ions, $\text{H}_3\text{O}^+(\text{H}_2\text{O})_n$ for $n = 1, 2, 3$ and 4 are dominated below 60 km, while NO^+ and O_2^+ are major ions above this altitude. In the chemistry of negative ions, water clusters, $\text{NO}_2^-(\text{H}_2\text{O})_n$ and $\text{CO}_3^-(\text{H}_2\text{O})_n$ for $n = 1$ and 2 are dominant ions below 40 km. Above this altitude electron plays an important role in the Martian ionosphere. The calculated values and positions of F and D peaks are in reasonable agreement with the occultation measurements made by Mars 4 and 5.

2. Input Data and Calculation

[4] Our previous paper represents the model calculation of electron densities above 100 km due to precipitation of solar wind electron in the nighttime ionosphere of Mars [Haider et al., 2002]. This model is extended now to calculate densities of positive ions, negative ions and electron between altitude 0 km and 220 km at interval 0.1 km due to precipitation of solar wind electron and galactic cosmic rays simultaneously. The high energy cosmic rays are propagated through the Martian atmosphere producing nucleonic cascades. The impact of primary cosmic rays onto the atmospheric gases produces protons, neutrons, and pions. Neutral pions quickly decay to gamma rays, and their contribution to the energy deposition is very important in the lower part of the atmosphere. Near mesosphere the maximum ion production rates are controlled by protons. The charged pions decay to muons, which do not decay before reaching the ground and the muon energy is transferred to the surface. The flux of incident cosmic rays is exponentially attenuated and is calculated between values 10^3 to 10^{-5} particles $\text{m}^{-2} \text{s}^{-1} \text{GeV}^{-1} \text{Ster}^{-1}$ at energy interval 1 to 1000 GeV [O'Brien et al., 1996]. The solar wind electron flux has been measured by Mars Global Surveyor at 340 km near solar zenith angle 106° [Haider et al., 2002]. The value of this flux decreases from 10^7 to 10^2 particles $\text{cm}^{-2} \text{s}^{-1} \text{eV}^{-1} \text{ster}^{-1}$ between energy 1 eV and 1000 eV. We have used these fluxes in the calculation of ion production rates and electron densities. The energy loss method for the calculation of ion production rates are given by Haider et al. [2002] and Vikas [2004]. These methods are described in section 3. The production rates of seven ions CO_2^+ , N_2^+ , Ar^+ , O_2^+ , CO^+ , O^+ and H_2O^+ are calculated by using these methods. The production rates have been used later in the continuity equation to calculate the ion and electron densities. Because of the fact that transport time is several orders of magnitude higher than chemical life time, we have neglected transport of ions in the present calculation.

[5] The neutral model atmosphere is taken as CO_2 , N_2 , N , Ar , O_2 , CO , H_2O , O_3 , O , NO , NO_2 and HNO_3 from various references [cf. Rodrigo et al., 1990; Nair et al., 1994; Owen et al., 1977; Haider et al., 2002; Vikas, 2004]. We have calculated density profiles of 34 ions under steady state chemical equilibrium condition. The electron density is calculated using charge neutrality condition. The chemical reactions and their rate coefficients are taken from Molina-Cuberos et al. [2002] and Haider et al. [2006]. These chemical reactions are given in Appendix A, where units are given in $\text{cm}^6 \text{s}^{-1}$ for trimolecular reaction and $\text{cm}^{-3} \text{s}^{-1}$ for bimolecular reactions. The reaction rates are given by one, two or three coefficients A, B, C, which represent $A \times$

$(T/300)^B \times \exp(-C/T)$. The convention is $3.7(-9) = 3.7 \times 10^{-9}$. Z represents an ion, which is not taken into account. The temperature is taken from Lopez-Valverde et al. [1998] and Bougher et al. [1999]. The rate coefficients for most three body reactions are measured using N_2 or O_2 as third body. We follow the convention of Molina-Cuberos et al. [2002], where CO_2 is assumed to have the same efficiency as O_2 or N_2 .

3. Methodology

3.1. Energy Loss Model

[6] Following Vikas [2004] the basic formula for energy loss per cm path into the material media by a particle traveling with the velocity V and undergoing inelastic collisions is written as:

$$\left(\frac{dE}{dh}\right)_{ion} = \frac{2\pi e^4}{m_0 V^2} NZ \left\{ \ln \left[\frac{m_0 V^2 E}{I^2 (1 - \beta^2)} \right] - \beta^2 \right\} \text{ergs/cm} \quad (1)$$

[7] For simplicity, it is convenient to introduce $m_0 V^2 = \beta^2 m_0 c^2$ and $E + m_0 c^2 = m_0 c^2 / \sqrt{1 - \beta^2}$, thus obtaining from equation (1)

$$\left(\frac{dE}{dh}\right)_{ion} = 4\pi r_0^2 \frac{m_0 c^2}{\beta^2} NZ \cdot \left\{ \ln \beta \left(\frac{E + m_0 c^2}{I} \right) \left(\frac{E}{m_0 c^2} \right)^{\frac{1}{2}} - \frac{1}{2} \beta^2 \right\} \text{MeV/cm} \quad (2)$$

where E is the energy; I is ionization potential; h is the height; r_0 is classical electron radius with $4\pi r_0^2 = 1.00 \times 10^{-24} \text{cm}^2/\text{electron}$; $\beta^2 = (V/c)^2 = 1 - [(E/m_0 c^2) + 1]^{-2}$; $m_0 c^2 = 0.51 \text{MeV}$ (rest energy of electron); N is the neutral density; Z is the atomic number and c is the velocity of light.

[8] Using equation (2), the ion production rate $P(\text{cm}^{-3} \text{s}^{-1})$ at height h and solar zenith angle χ is given below:

$$p(h, \chi) = \frac{1}{Q} \int_E \int_{\Omega} (dE/dh) F(\chi, E, \Omega) d\Omega dE \quad (3)$$

where $Q = 35 \text{eV}$ is the energy required for the formation of an electron ion pair; χ is taken as 105° and F is the total differential flux of the galactic cosmic rays being expressed in $\text{cm}^{-2} \text{s}^{-1} \text{GeV}^{-1} \text{ster}^{-1}$ at height h and Ω is the spatial angle. The flux of galactic cosmic rays is adopted from O'Brien et al. [1996]. Since the cosmic rays penetrate isotropically into the atmosphere, equation (3) reduces as follows:

$$p(h, \chi) = \frac{2\pi}{Q} \int (dE/dh) F(\chi, E) dE \quad (4)$$

3.2. Analytical Yield Spectrum Model

[9] Analytical yield spectrum model is based on Monte Carlo technique. In this method mono energetic electrons of different incident energies were introduced in a gas medium at some pitch angle. This method includes elastic and inelastic collision between electrons and neutral species, electron-electron Coulomb collisions and pitch angle and

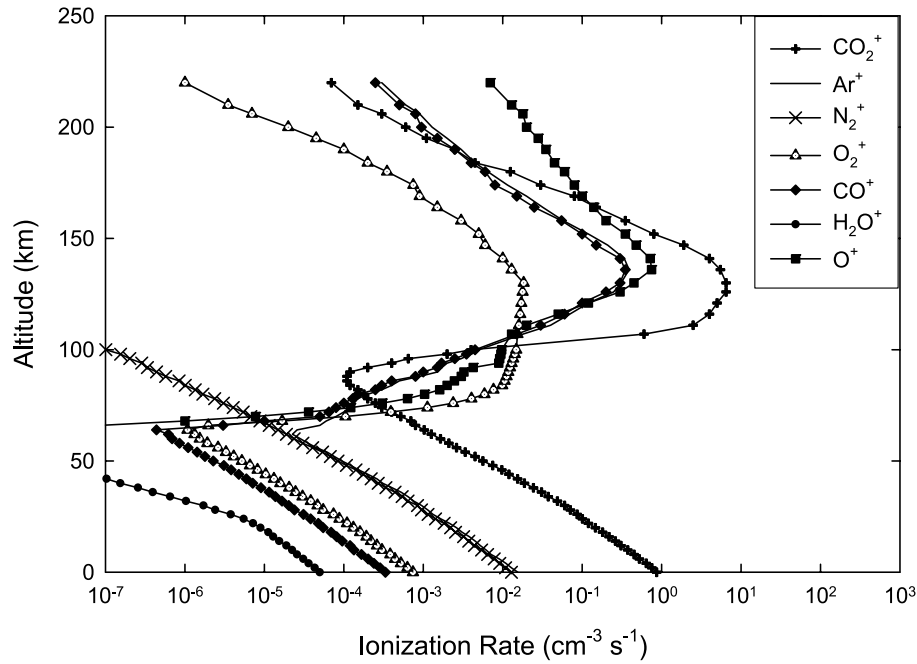


Figure 1. Ionization rates of CO_2^+ , Ar^+ , N_2^+ , O_2^+ , CO^+ , H_2O^+ and O^+ due to impact of solar wind electron and galactic cosmic rays with the atmosphere of Mars at solar zenith angle 105° .

finite gyro radius effects of electrons. The scattering due to electron-ion interaction was neglected. In the simulation the probabilities were computed for various types of collisions to occur during an element dS of path length. This path length is always considerably shorter than mean free path for elastic collision. A real number between 0 and 1.0 called from a random generator determined whether a collision took place or not. If not, the amount of energy lost through Coulomb losses to the ambient electron was calculated from Butler-Buckingham formula [Dalgarno *et al.*, 1963] and was added to the accumulated energy loss. If the collision with atmospheric gases occurred, a further decision was to consider whether the collision was elastic or inelastic. For the elastic collision the scattering angle calculation was carried out by Porter and Jump [1978]. If the scattering event is inelastic, then the excited/ionized state is calculated from Jackman *et al.* [1977]. It is assumed that electrons are ejected isotropically. Using this method, the energy of secondary or tertiary electrons and their positions were calculated at that time when primary solar wind electrons ionize the atmospheric constituents. In this way a yield spectrum function was generated for the calculation of the yield of any state in the mixture of gases. The function was fitted analytically later. The yield spectra were presented in terms of two, three, four and five dimensional functions [cf. Seth *et al.*, 2002; Haider *et al.*, 2002; Haider *et al.*, 2006; Seth *et al.*, 2006a, 2006b] We have used three dimensional yield spectra to calculate the ionization rate due to solar wind electron impact on Martian atmosphere as given below:

$$q(h) = \int_w^\infty dE_o \int_w^E U^c(E, Z, E_o) \rho(h) p_i(E) \phi(E_o) dE \quad (5)$$

where i refers to source gas, p_i is the ionization probability, $U^c(E, Z, E_o)$ is the three dimensional composite yield spectrum approach, $\rho(h)$ is the mass density and $\phi(E_o)$ is the solar wind electron spectra of incident energy E_o observed by electron reflectometer experiment onboard Mars Global Surveyor. The value of this energy flux is taken from Seth *et al.* [2002]. The ionization probability is calculated by

$$p_i(E) = C_i (1 - \epsilon_i^{-\alpha_i})^{\gamma_i} \epsilon_i^{-u_i} \quad (6)$$

where $\epsilon_i = E/I_i$, I_i being lowest ionization threshold. The parameters C_i , α_i , γ_i and u_i are taken in equation (6) from Haider [1999] for Martian gases. Variable Z in equation (5) is connected with h by following relation

$$Z(h) = \frac{1}{R} \int_0^\infty \frac{\rho(h)}{\cos \theta} dh \quad (7)$$

with a mean scale factor R defined by

$$R = R_o (E_o/E_o 1000)^q + \tau \quad (8)$$

The parameters R_o , τ and q in equation (8) are given by Singhal and Green [1981] and Green and Singhal [1979].

4. Results and Discussion

[10] In Figure 1 we have represented total ion production rates of seven ions CO_2^+ , N_2^+ , Ar^+ , O_2^+ , CO^+ , H_2O^+ , and O^+ due to impact of solar wind electron and galactic cosmic rays with the atmospheric gases. As expected, solar wind electron is the major source above 70 km, while the ionization produced by galactic cosmic rays dominates below this altitude. The total ion production rates are

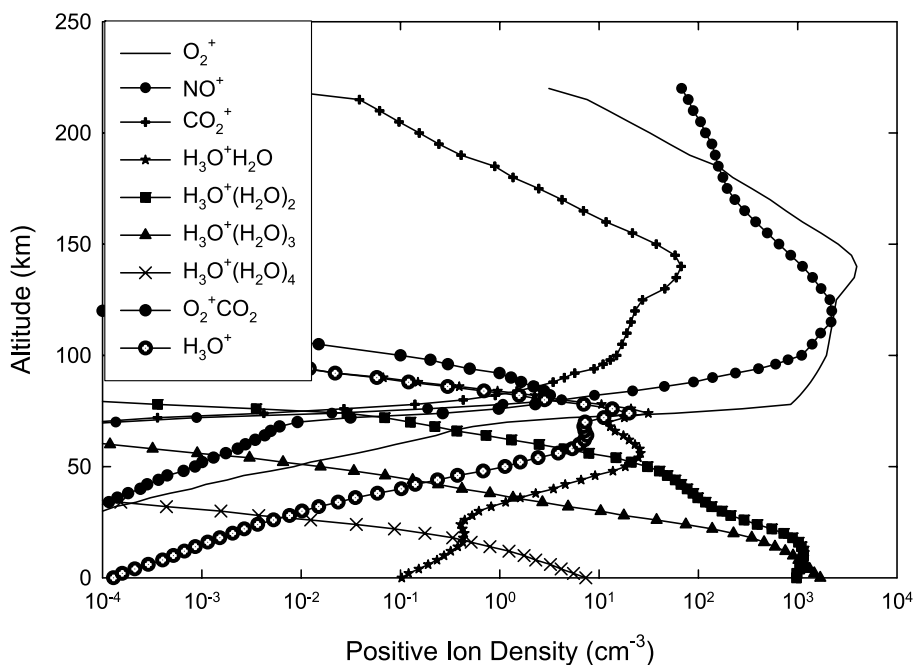


Figure 2. Positive ion densities of O_2^+ , NO^+ , CO_2^+ , $H_3O^+H_2O$, $H_3O^+(H_2O)_2$, $H_3O^+(H_2O)_3$, $H_3O^+(H_2O)_4$, $O_2^+CO_2$ and H_3O^+ due to impact of solar wind electron and galactic cosmic rays with the atmosphere of Mars at solar zenith angle 105° .

obtained by adding solar wind electron impact and galactic cosmic ray ionizations. The production rates of ions Ar^+ and H_2O^+ are significantly low above 70 km due to impact of solar wind electron.

[11] In Figure 2 we present the number density of nine major positive ions, O_2^+ , NO^+ , CO_2^+ , $H_3O^+H_2O$, $H_3O^+(H_2O)_2$, $H_3O^+(H_2O)_3$, $H_3O^+(H_2O)_4$, $O_2^+CO_2$ and H_3O^+ . The major ion CO_2^+ is produced initially due to impact of solar wind electron and galactic cosmic rays with the nighttime atmosphere of Mars. Above 80 km, CO_2^+ is quickly removed by atomic oxygen leading to O_2^+ as a dominant ion. The other major ion NO^+ is formed due to destruction of O_2^+ with NO. These ions are entirely destroyed by dissociative recombination reaction. The peaks of O_2^+ and NO^+ are broad and located at altitudes ~ 130 km and 120 km respectively. In this region, the densities of O_2^+ and NO^+ are approximately related as $[O_2^+] \propto [CO_2^+][O]/[N_e]$ and $[NO^+] \propto [O_2^+][NO]/[N_e]$ respectively, where $[CO_2^+]$ and $[N_e]$ are the ion and electron densities respectively. At altitude range ~ 60 to 80 km, the ion $O_2^+CO_2$ is produced due to three body reaction, which is fully destroyed by water vapor in the formation of H_3O^+ . Below 60 km, nearly all H_3O^+ ions are lost by three body reaction in the formation of hydrated ions $H_3O^+(H_2O)_n$, for $n = 1, 2, 3$ and 4. Once $H_3O^+H_2O$ ion has been produced, water vapor molecules are associated into it. We have considered the reactions of production and loss to form cluster ions up to four water molecules. In this region the dissociative recombination of $H_3O^+(H_2O)_n$ are always smaller than other loss processes.

[12] In Figure 3 we present number densities of eight major negative ions (CO_4^- , CO_3^- , $CO_3^-H_2O$, $CO_3^-(H_2O)_2$, $NO_2^-H_2O$, $NO_2^-(H_2O)_2$, $NO_3^-H_2O$ and $NO_3^-(H_2O)_2$) and electron. In the chemistry of negative ions, water cluster

of CO_3^- and NO_2^- (i.e., $CO_3^-(H_2O)_n$, $NO_2^-(H_2O)_n$ for $n = 1$ and 2) are dominant ions below 40 km. Above this altitude electron plays an important role in the nighttime ionosphere of Mars. The relative high abundance of oxygen bearing molecules permits the presence of negative ions in the lower ionosphere. Initially, negative ions O^- and O_2^- are produced through electron capture by ozone and molecular oxygen. Later CO_3^- and CO_4^- are produced from three body reactions $O^- + CO_2 + M \rightarrow CO_3^- + M$ and $O_2^- + CO_2 + M \rightarrow CO_4^- + M$. The ion CO_4^- is destroyed by atomic oxygen producing CO_3^- whose peak occurs at about 25 km. The loss of CO_3^- with H_2O is the major source of production of $CO_3^-H_2O$ and $CO_3^-(H_2O)_2$, which is entirely destroyed by dissociation. The ion CO_3^- is also destroyed by NO and NO_2 forming NO_2^- and NO_3^- respectively. Later NO_2^- and NO_3^- are hydrated by three body reaction with water vapor producing $NO_2^-(H_2O)_n$ and $NO_3^-(H_2O)_n$, which are dissociated by neutral collisions. Below 40 km, these reactions are important for the production of nearly 100% $CO_3^-(H_2O)_2$ ion. The ion $CO_3^-H_2O$ is partially destroyed by NO to produce second major ion $NO_2^-H_2O$. In Figures 2 and 3, we have not plotted the number densities of minor ions, Ar^+ , H_3O^+HO , $CO_2^+CO_2$, CO^+ , N_2^+ , NO^+CO_2 , $O_2^+(CO_2)_2$, $O_2^+H_2O$, $O_2^+(H_2O)_2$, O_4^+ , O^+ , NO_2^- , NO_3^- , O_2^- , O_3^- and O^- because of their low values.

[13] Seth *et al.* [2002] and Haider *et al.* [2002] have shown that solar wind electron fluxes measured by electrostatic analyzer experiment carried aboard Mars Global Surveyor, are of right magnitude to cause the sufficient impact ionization in the upper ionosphere for the measured nighttime electron densities. Molina-Cuberos *et al.* [2002] have shown that galactic cosmic rays are the major source of nighttime ionization in the lower ionosphere of Mars. We have used both sources of ionization in our model to

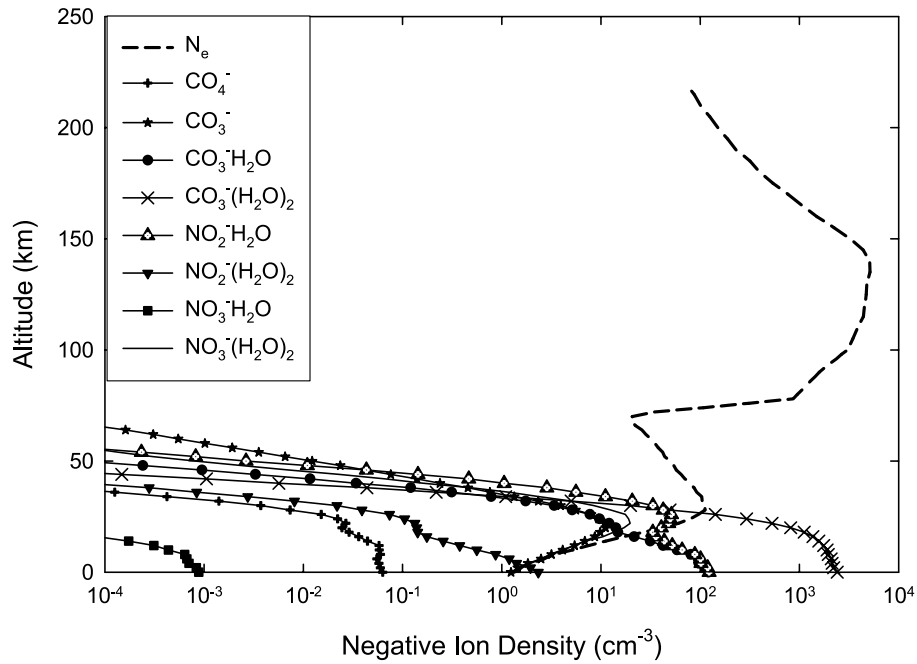


Figure 3. Negative ion densities of electron, CO_4^- , CO_3^- , $\text{CO}_3^-\text{H}_2\text{O}$, $\text{CO}_3^-(\text{H}_2\text{O})_2$, $\text{NO}_2^-\text{H}_2\text{O}$, $\text{NO}_2^-(\text{H}_2\text{O})_2$, $\text{NO}_3^-\text{H}_2\text{O}$ and $\text{NO}_3^-(\text{H}_2\text{O})_2$ due to impact of solar wind electron and galactic cosmic rays with the atmosphere of Mars at solar zenith angle 105° .

calculate the ion and electron density. It is found that impact ionization caused by solar wind electron and galactic cosmic rays produces maximum electron density $\sim 5.2 \times 10^3 \text{ cm}^{-3}$ and $\sim 100 \text{ cm}^{-3}$ at altitudes 130 km and 30 km respectively. These results are in good agreement with the model calculations of Haider et al. [2002] and Molina-

Cuberos et al. [2002] as far as the position and value of peak electron density are concerned.

[14] In Figure 4, calculated total ion density is compared with the observations at nearly same areophysical condition. The nighttime ionosphere has been observed above the surface of Mars from Mars 4 and Mars 5 on 10 and 18

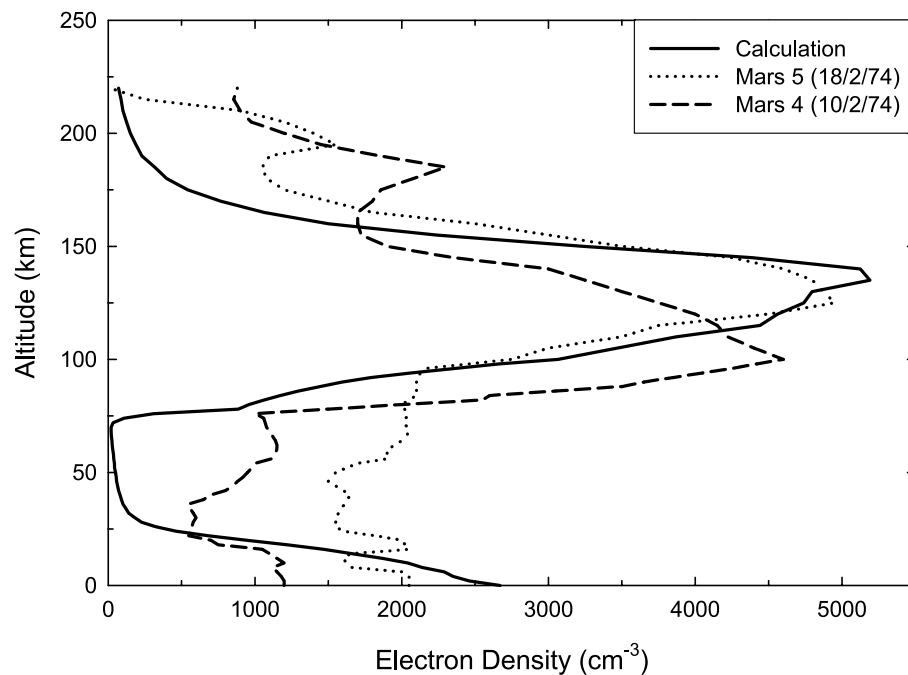


Figure 4. Calculated electron density (total negative ion density) profile is represented at solar zenith angle 105° . The electron densities measured by Mars 4 and Mars 5 at solar zenith angle 106° are also plotted in this figure.

Table 1.

| | Peak Densities | | | Peak Heights | | |
|--------|------------------------------|-------------------------------------|-------------------------------------|----------------|-----------------------|-----------------------|
| | Calculated, cm^{-3} | Measured (Mars 4), cm^{-3} | Measured (Mars 5), cm^{-3} | Calculated, km | Measured (Mars 4), km | Measured (Mars 5), km |
| F peak | 5.2×10^3 | 4.6×10^3 | 5.0×10^3 | ~ 130 | 110 | 130 |
| D peak | 1.0×10^2 | $\sim 1.2 \times 10^3$ | $\sim 2.0 \times 10^3$ | 30 | $\sim 15-20$ | ~ 25 |

February 1974 [Savich and Samovol, 1976]. These observations were carried out by radio occultation experiment in spring season at coordinate 38°N 214°W and local time 0430 with solar zenith angle 106° during low solar activity period. It appears that these measurements contain three peaks at altitude ranges 180–200 km, 110–130 km and 30–35 km, which were produced by different physical processes. The first layer at $\sim 180-200$ km may exist primarily due to transport of photoelectrons and ions from the dayside ionosphere, which recombined with the nighttime ionosphere across the terminator [cf. Fox et al., 1993]. The second major peak has observed the electron concentration $\sim 5.0 \times 10^3 \text{ cm}^{-3}$, which can not be considered as the decay of dayside ionosphere. The decrease of electron concentration after sunset is characterized by the time constant $\tau = 1/\alpha N_o$, where N_o is the value of electron concentration at the moment of ‘switch off’ the source of ionization and $\alpha = 2.55 \times 10^{-7} \text{ cm}^3 \text{ s}^{-1}$ [Mul and McGowan, 1979] is the effective recombination coefficient. If we take least value of $N_o \sim 10^4 \text{ cm}^{-3}$ from the top of the daytime ionosphere [Haider et al., 2006], τ is about 400 second. It is obvious that with this value of τ , the ionospheric plasma must have completely disappeared several hours after sunset. Thus it is necessary to consider the presence of an additional source of ionization, not connected directly with solar radiation to explain the existence of second peak in the nighttime ionosphere.

[15] We have reproduced this peak due to solar wind electron impact ionization. This calculation shows good agreement with the measurement made by Mars 5. However, the calculated peak height is increased by 20 km from the observation carried by Mars 4. This difference can be related to various reasons: (1) If the peak of electron density on 10 February 1974 is caused by more energetic electrons, it should be located a few tens of kilometers lower than the calculated peak, (2) A global dust storm could change the measured peak height by 20–30 km due to heating effects in lower thermosphere of Mars [Kliore et al., 1973; Martin, 1984; Verigin et al., 1991] and (3) the scale height of the topside Martian ionosphere is unusually sensitive to the variations of solar activity. Both of last two effects can lead to the variation of the density distribution in thermosphere, so that neutral gas density ($\text{CO}_2 \sim 10^9 \text{ cm}^{-3}$) corresponding to the peak ionization rate is at different height during different observational period.

[16] Each measured profiles show the existence of plasma at height below 80 km with a small shoulder of electron density between $\sim 1 \text{ cm}^{-3}$ and $2 \times 10^3 \text{ cm}^{-3}$ at altitude ~ 30 km. This signature is not very prominent and other published Mars low altitude profiles do not show similar features [Zhang et al., 1990]. The lower electron peak at altitude ~ 30 km is not seen in the estimated value of total ion density because the density of CO_3^- (H_2O) $_2$ is larger by

several order of magnitudes from electron density in this altitude region. There has been found that calculated plasma densities are smaller by factors 5 and 15 than those measured by Mars 4 and Mars 5 respectively. Our low values of plasma density could be explained by large precipitation of galactic cosmic rays in the nighttime ionosphere of Mars. The present calculation is made using galactic cosmic ray population of fluxes 10^3 to 10^{-5} particle $\text{m}^{-2} \text{ s}^{-1} \text{ GeV}^{-1} \text{ ster}^{-1}$ for energy range 1–1000 GeV. We do not know what fraction of galactic cosmic rays actually precipitate in the nighttime atmosphere of Mars. Another reason could be associated with the error of measurements. The presence of plasma in the lower ionosphere is derived on the basis of the formal inversion of the set of observations in symmetrical approximation. During the occultation measurements, the possible displacement of electron density due to this error was estimated to be $\approx \pm 500 \text{ cm}^{-3}$ [Savich and Samovol, 1976]. This could be an important reason for difference between calculation and measurement at low ionospheric region.

[17] The nighttime ionosphere of Earth is divided into D, E and F regions. The D region is formed at $\sim 65-70$ km due to precipitation of galactic cosmic rays. Sporadic E layer represents maximum ionization at $\sim 105-110$ km due to metallic ions. The F peak is produced by the precipitation of magnetospheric electrons. By analogy to Earth’s ionosphere, we suggest that Martian ionosphere consists D and F layers in the nighttime ionosphere. The chemistry of meteoric ions (Ca^+ , Mg^+ and Fe^+) is not included in our model. Therefore E layer is not seen in Figure 4. The preliminary calculations of Pesnell and Grebowsky [2000] have reported that the metal ion layer exists at about 80 km in the lower ionosphere of Mars. We have also experimental evidence for the tentative identification of ion Mg^+CO_2 in Thermal Emission Spectrometer data [Aikin and Maguire, 2005]. The calculated and measured peak densities and peak heights are given in Table 1.

5. Conclusions

[18] In this paper we have calculated production rates, loss rates, positive ion and negative ion densities between altitudes 0 km and 220 km due to precipitation of solar wind electron and galactic cosmic rays in the nighttime ionosphere of Mars at solar zenith angle $\sim 105^\circ$. These calculations are compared with the occultation measurements carried by Mars 4 and Mars 5 above the dark surface of Mars. These observations have detected major peak between altitudes ~ 110 km and 130 km. They did not detect clear peak below 80 km. However, a small shoulder is seen in these measurements at altitude region $\sim 15-25$ km. The existence of this plasma features needs further experimental verification. These peaks are represented as F and D layers similar to that observed in Earth’s ionosphere. The present

Table A1. Chemical Reactions

| Positive ions | |
|--|--|
| $\text{Ar}^+ + \text{CO}_2 \rightarrow \text{CO}_2^+ + \text{Ar}$ | 4.20(-10) |
| $\text{Ar}^+ + \text{N}_2 \rightarrow \text{N}_2^+ + \text{Ar}$ | 2.50(-12) |
| $\text{Ar}^+ + \text{O}_2 \rightarrow \text{O}_2^+ + \text{Ar}$ | 5.50(-11) |
| $\text{CO}_2^+ + \text{O} \rightarrow \text{O}^+ + \text{CO}_2$ | 1.00(-10) |
| $\text{CO}_2^+ + \text{O} \rightarrow \text{O}_2^+ + \text{CO}$ | 1.64(-10) |
| $\text{CO}_2^+ + \text{N} \rightarrow \text{NO}^+ + \text{CO}$ | 1.00(-11) |
| $\text{CO}_2^+ + \text{N} \rightarrow \text{CO}^+ + \text{NO}$ | 1.00(-11) |
| $\text{CO}_2^+ + \text{NO} \rightarrow \text{NO}^+ + \text{CO}_2$ | 1.20(-10) |
| $\text{CO}_2^+ + \text{CO} \rightarrow \text{CO}^+ + \text{CO}_2$ | 1.90(-12) |
| $\text{CO}_2^+ + \text{CO}_2 + \text{M} \rightarrow \text{CO}_2^+\text{CO}_2 + \text{M}$ | 2.50(-28) |
| $\text{CO}_2^+ + \text{O}_2 \rightarrow \text{O}_2^+ + \text{CO}_2$ | 1.00(-10) |
| $\text{CO}_2^+\text{CO}_2 + \text{O}_2 \rightarrow \text{O}_2^+ + \text{CO}_2 + \text{CO}_2$ | 1.53(-10) |
| $\text{CO}_2^+\text{CO}_2 + \text{O}_2 \rightarrow \text{O}_2^+\text{CO}_2 + \text{CO}_2$ | 2.70(-11) |
| $\text{CO}^+ + \text{CO}_2 \rightarrow \text{CO}_2^+ + \text{CO}$ | 1.42(-9) |
| $\text{CO}^+ + \text{O} \rightarrow \text{CO} + \text{O}^+$ | 1.40(-10) |
| $\text{CO}^+ + \text{NO} \rightarrow \text{CO} + \text{NO}^+$ | 3.30(-10) |
| $\text{H}_3\text{O}^+ + \text{H}_2\text{O} + \text{M} \rightarrow \text{H}_3\text{O}^+\text{H}_2\text{O} + \text{M}$ | 3.40(-27) |
| $\text{H}_3\text{O}^+\text{HO} + \text{H}_2\text{O} \rightarrow \text{H}_3\text{O}^+\text{H}_2\text{O} + \text{OH}$ | 1.40(-9) |
| $\text{H}_3\text{O}^+\text{H}_2\text{O} + \text{H}_2\text{O} + \text{M} \rightarrow \text{H}_3\text{O}^+(\text{H}_2\text{O})_2 + \text{M}$ | 2.30(-27) |
| $\text{H}_3\text{O}^+\text{H}_2\text{O} + \text{M} \rightarrow \text{H}_3\text{O}^+ + \text{H}_2\text{O} + \text{M}$ | 7.00(-26) |
| $\text{H}_3\text{O}^+(\text{H}_2\text{O})_2 + \text{H}_2\text{O} + \text{M} \rightarrow \text{H}_3\text{O}^+(\text{H}_2\text{O})_3 + \text{M}$ | 2.40(-27) |
| $\text{H}_3\text{O}^+(\text{H}_2\text{O})_2 + \text{M} \rightarrow \text{H}_3\text{O}^+\text{H}_2\text{O} + \text{H}_2\text{O} + \text{M}$ | 7.00(-18) |
| $\text{H}_3\text{O}^+(\text{H}_2\text{O})_3 + \text{H}_2\text{O} + \text{M} \rightarrow \text{H}_3\text{O}^+(\text{H}_2\text{O})_4 + \text{M}$ | 9.00(-28) |
| $\text{H}_3\text{O}^+(\text{H}_2\text{O})_3 + \text{M} \rightarrow \text{H}_3\text{O}^+(\text{H}_2\text{O})_2 + \text{H}_2\text{O} + \text{M}$ | 4.00(-14) |
| $\text{H}_3\text{O}^+(\text{H}_2\text{O})_4 + \text{M} \rightarrow \text{H}_3\text{O}^+(\text{H}_2\text{O})_3 + \text{H}_2\text{O} + \text{M}$ | 6.00(-12) |
| $\text{N}_2^+ + \text{CO} \rightarrow \text{CO}^+ + \text{N}_2$ | 7.40(-11) |
| $\text{N}_2^+ + \text{CO}_2 \rightarrow \text{CO}_2^+ + \text{N}_2$ | 7.70(-10) |
| $\text{N}_2^+ + \text{O}_2 \rightarrow \text{O}_2^+ + \text{N}_2$ | 6.00(-11) |
| $\text{O}^+ + \text{CO}_2 \rightarrow \text{O}_2^+ + \text{CO}$ | 1.00(-9) |
| $\text{O}^+ + \text{O}_2 \rightarrow \text{O}_2^+ + \text{O}$ | $2.00(-11) \times (300/T)^{0.55}$ |
| $\text{O}^+ + \text{N}_2 \rightarrow \text{NO}^+ + \text{N}$ | 1.20(-12) |
| $\text{O}_2^+ + \text{CO}_2 + \text{M} \rightarrow \text{O}_2^+\text{CO}_2 + \text{M}$ | 1.70(-29) |
| $\text{O}_2^+ + \text{H}_2\text{O} + \text{M} \rightarrow \text{O}_2^+\text{H}_2\text{O} + \text{M}$ | 2.80(-28) |
| $\text{O}_2^+ + \text{NO} \rightarrow \text{NO}^+ + \text{O}_2$ | 4.40(-10) |
| $\text{O}_2^+ + \text{O}_2 + \text{M} \rightarrow \text{O}_4^+ + \text{M}$ | 1.00(-30) |
| $\text{O}_2^+ + \text{N} \rightarrow \text{NO}^+ + \text{O}$ | 1.20(-10) |
| $\text{O}_2^+\text{CO}_2 + \text{CO}_2 \rightarrow \text{O}_2^+ + 2\text{CO}_2$ | 2.40(-13) |
| $\text{O}_2^+ + \text{N}_2 + \text{M} \rightarrow \text{O}_2^+\text{N}_2 + \text{M}$ | 8.00(-31) |
| $\text{O}_2^+ + \text{N}_2 \rightarrow \text{NO}^+ + \text{NO}$ | 5.00(-16) |
| $\text{O}_2^+\text{N}_2 + \text{H}_2\text{O} \rightarrow \text{O}_2^+\text{H}_2\text{O} + \text{N}_2$ | 4.00(-9) |
| $\text{O}_2^+\text{N}_2 + \text{N}_2 \rightarrow \text{O}_2^+ + 2\text{N}_2$ | 2.00(-11) |
| $\text{O}_2^+\text{N}_2 + \text{O}_2 \rightarrow \text{O}_4^+ + \text{N}_2$ | 5.00(-11) |
| $\text{O}_2^+\text{CO}_2 + \text{CO}_2 + \text{M} \rightarrow \text{O}_2^+(\text{CO}_2)_2 + \text{M}$ | 5.00(-30) |
| $\text{O}_2^+\text{CO}_2 + \text{H}_2\text{O} \rightarrow \text{O}_2^+\text{H}_2\text{O} + \text{CO}_2$ | 1.00(-9) |
| $\text{O}_2^+(\text{CO}_2)_2 + \text{H}_2\text{O} \rightarrow \text{Z}$ | 2.30(-9) |
| $\text{O}_2^+\text{H}_2\text{O} + \text{H}_2\text{O} \rightarrow \text{H}_3\text{O}^+ + \text{HO} + \text{O}_2$ | 2.04(-10) |
| $\text{O}_2^+\text{H}_2\text{O} + \text{H}_2\text{O} \rightarrow \text{H}_3\text{O}^+\text{HO} + \text{O}_2$ | 9.96(-10) |
| $\text{O}_2^+\text{H}_2\text{O} + \text{H}_2\text{O} + \text{M} \rightarrow \text{O}_2^+(\text{H}_2\text{O})_2 + \text{M}$ | 1.30(-27) |
| $\text{O}_2^+(\text{H}_2\text{O})_2 + \text{H}_2\text{O} \rightarrow \text{Z}$ | 3.24(-10) |
| $\text{O}_4^+ + \text{CO}_2 \rightarrow \text{O}_2^+\text{CO}_2 + \text{O}_2$ | 4.00(-13) |
| $\text{O}_4^+ + \text{H}_2\text{O} \rightarrow \text{O}_2^+\text{H}_2\text{O} + \text{O}_2$ | 1.70(-9) |
| $\text{NO}^+ + \text{CO}_2 + \text{M} \rightarrow \text{NO}^+\text{CO}_2 + \text{M}$ | $1.4(-29) \times (300/T)^{4.0}$ |
| $\text{NO}^+\text{CO}_2 + \text{M} \rightarrow \text{NO}^+ + \text{CO}_2 + \text{M}$ | $3.1(+4) \times (T)^{-4.0} \exp(-4590/T)$ |
| $\text{CO}_2^+ + \text{e} \rightarrow \text{CO} + \text{O}$ | 1.40(-4)/Te |
| $\text{NO}^+ + \text{e} \rightarrow \text{N} + \text{O}$ | $2.30(-7) \times (300/\text{Te})^{0.5}$ |
| $\text{CO}^+ + \text{e} \rightarrow \text{C} + \text{O}$ | $2.00(-7) \times (300/\text{Te})^{0.48}$ |
| $\text{O}^+ + \text{e} \rightarrow \text{O}$ | $4.00(-12) \times (300/T)^{0.7}$ |
| $\text{H}_3\text{O}^+\text{HO} + \text{e} \rightarrow \text{Neutral}$ | 1.50(-6) |
| $\text{H}_3\text{O}^+ + \text{e} \rightarrow \text{H}_2 + \text{OH}$ | 2.33(-7) |
| $\text{H}_3\text{O}^+ + \text{e} \rightarrow \text{H} + \text{OH} + \text{H}$ | 2.33(-7) |
| $\text{H}_3\text{O}^+ + \text{e} \rightarrow \text{H}_2\text{O} + \text{H}$ | 2.34(-7) |
| $\text{O}_2^+\text{H}_2\text{O} + \text{e} \rightarrow \text{H}_2\text{O} + \text{O}_2$ | 2.00(-6) |
| $\text{O}_2^+\text{CO}_2 + \text{e} \rightarrow \text{O}_2 + \text{CO}_2$ | 4.00(-6) |
| $\text{N}_2^+ + \text{e} \rightarrow \text{N} + \text{N}$ | $3.50(-7) \times (300/T)^{0.5}$ |
| $\text{O}_2^+\text{N}_2 + \text{e} \rightarrow \text{O}_2 + \text{N}_2$ | $1.95(-7) \times (300/T)^{0.7}$ |
| $\text{O}_2^+ + \text{e} \rightarrow \text{O} + \text{O}$ | $4.20(-7) \times (300/T)^n \quad 0.37 < n < 0.9$ |
| $\text{O}_2^+\text{O}_2 + \text{e} \rightarrow \text{O}_2 + \text{O}_2$ | $4.20(-6) \times (300/T)^{0.48}$ |
| $\text{H}_3\text{O}^+\text{H}_2\text{O} + \text{e} \rightarrow \text{Neutral}$ | 2.20(-6) |
| $\text{H}_3\text{O}^+(\text{H}_2\text{O})_2 + \text{e} \rightarrow \text{Neutral}$ | 3.80(-6) |
| $\text{H}_3\text{O}^+(\text{H}_3\text{O})_3 + \text{e} \rightarrow \text{Neutral}$ | 4.90(-6) |
| $\text{H}_3\text{O}^+(\text{H}_3\text{O})_4 + \text{e} \rightarrow \text{Neutral}$ | 6.00(-6) |
| $\text{X}^+ + \text{X}^- \rightarrow \text{Neutral}$ | 6.00(-8) |

Table A1. (continued)

| Negative ions | |
|--|--------------------|
| $e + O \rightarrow O^- + h$ | 1.30(-15) |
| $e + O_2 + M \rightarrow O_2^- + M + h$ | 2.00(-31), 1, -600 |
| $e + O_3 \rightarrow O^- + O_2$ | 9.10(-12), -1.46 |
| $O^- + CO_2 + M \rightarrow CO_3^- + M$ | 1.10 (-27) |
| $O_2^- + CO_2 + M \rightarrow CO_4^- + M$ | 1.30(-29) |
| $O_2^- + O \rightarrow O^- + O_2$ | 1.50(-10) |
| $O_2^- + O_3 \rightarrow O_3^- + O_2$ | 7.80(-10) |
| $O_2^- + O_2 + M \rightarrow O_4^- + M$ | 3.40(-31) |
| $O_2^- + NO_2 \rightarrow NO_2^- + O_2$ | 7.00(-10) |
| $O_3^- + O \rightarrow 2O_2 + e$ | 1.00(-10) |
| $O_3^- + O \rightarrow O_2^- + O_2$ | 2.50(-10) |
| $O_3^- + NO \rightarrow NO_3^- + O$ | 2.60(-12) |
| $O_3^- + NO_2 \rightarrow NO_3^- + O_2$ | 2.80(-10) |
| $O_3^- + CO_2 \rightarrow CO_3^- + O_2$ | 5.50(-10) |
| $O_4^- + O \rightarrow O_3^- + O_2$ | 4.00(-10) |
| $O_4^- + CO_2 \rightarrow CO_4^- + O_2$ | 4.30(-10) |
| $O_4^- + NO \rightarrow NO_3^- + O_2$ | 2.50(-10) |
| $CO_3^- + NO \rightarrow NO_2^- + CO_2$ | 1.10(-11) |
| $CO_3^- + NO_2 \rightarrow NO_3^- + CO_2$ | 2.00(-10) |
| $CO_3^- + H_2O + M \rightarrow CO_3^- H_2O + M$ | 1.00(-28) |
| $CO_3^- + O_2 \rightarrow O_3^- + CO_2$ | 6.00(-15) |
| $CO_3^- H_2O + M \rightarrow CO_3^- + H_2O + M$ | 7.20(-4), 1, -7050 |
| $CO_3^- H_2O + NO_2 \rightarrow NO_3^- + CO_2 + H_2O$ | 1.50(-10) |
| $CO_3^- H_2O + NO \rightarrow NO_2^- + CO_2 + H_2O$ | 3.50(-12) |
| $CO_3^- H_2O + NO \rightarrow NO_2^- H_2O + CO_2$ | 3.50(-12) |
| $CO_3^- (H_2O) + H_2O + M \rightarrow CO_3^- (H_2O)_2 + M$ | 1.00(-28) |
| $CO_3^- (H_2O)_2 + M \rightarrow CO_3^- (H_2O) + H_2O + M$ | 6.50(-3), 1, -6800 |
| $CO_4^- + NO \rightarrow NO_3^- + CO_2$ | 4.80(-11) |
| $CO_4^- + O \rightarrow CO_3^- + O_2$ | 1.40(-10) |
| $CO_4^- + O_3 \rightarrow O_3^- + CO_2 + O_2$ | 1.30(-10) |
| $NO_2^- + O_3 \rightarrow NO_3^- + O_2$ | 1.20(-10) |
| $NO_2^- + NO_2 \rightarrow NO_3^- + NO$ | 2.0(-13) |
| $NO_2^- + H_2O + M \rightarrow NO_2^- H_2O + M$ | 1.60(-28) |
| $NO_2^- H_2O + H_2O + M \rightarrow NO_2^- (H_2O)_2 + M$ | 3.80(-29) |
| $NO_2^- H_2O + M \rightarrow NO_2^- + H_2O + M$ | 5.70(-4), 1, -7600 |
| $NO_2^- (H_2O)_2 + M \rightarrow NO_2^- H_2O + H_2O + M$ | 5.80(-14) |
| $NO_3^- + H_2O + M \rightarrow NO_3^- H_2O + M$ | 1.60(-28) |
| $NO_3^- + CO_2 \rightarrow CO_3^- + NO$ | 1.00(-11) |
| $NO_3^- + O \rightarrow NO_2^- + O_2$ | <1.0(-11) |
| $NO_3^- + O_3 \rightarrow NO_2^- + 2O_2$ | 1.00(-13) |
| $NO_3^- + NO \rightarrow NO_2^- + NO_2$ | 1.00(-12) |
| $NO_3^- H_2O + M \rightarrow NO_3^- + H_2O + M$ | 1.00(-3), 1, -7300 |
| $NO_3^- H_2O + H_2O + M \rightarrow NO_3^- (H_2O)_2 + M$ | 1.60(-28) |
| $NO_3^- H_2O + HNO_3 \rightarrow NO_3^- HNO_3 + H_2O$ | >5.0(-10) |
| $NO_3^- (H_2O)_2 + M \rightarrow NO_3^- H_2O + H_2O + M$ | 1.50(-2), 1, -7150 |

calculation suggests that solar wind electron produces F peak at altitude ~ 130 km, while D peak is produced by galactic cosmic rays at altitude ~ 30 km. The ion density is not measured in the nighttime ionosphere of Mars. In absence of these measurements our calculation can be used as a diagnostic tool for future design of density payloads and for the subsequent data analysis to confirm the presence of D region in the lower atmosphere of Mars.

Appendix A

[19] See Table A1.

[20] **Acknowledgments.** The authors are grateful to Gregorio J. Molina-Cuberos for his discussion in preparing this paper.

[21] Amitava Bhattacharjee thanks the reviewers for their assistance in evaluating this paper.

References

- Aikin, A. C., and W. C. Maguire (2005), Detection of Mg+CO₂ ion produced via meteoritic material in the Martian atmosphere, Presented in DPS meeting.
- Bougher, S. W., S. Engel, R. G. Roble, and B. Foster (1999), Comparative terrestrial planet thermosphere 2, Solar cycle variation of global structure and winds at equinox, *J. Geophys. Res.*, *104*, 16,591–16,611.
- Dalgarno, A., B. M. McElroy, and R. J. Moffett (1963), Electron temperature in the ionosphere, *Planet. Space Sci.*, *11*, 463–470.
- Fjeldbo, G., A. Kliore, and B. Seidel (1970), The Mariner 1969 occultation measurements of the upper atmosphere of Mars, *Radio Sci.*, *5*, 381–386.
- Fjeldbo, G., et al. (1977), Viking radio occultation measurements of Martian atmosphere and topography: Primary mission covering age, *J. Geophys. Res.*, *82*, 4317–4324.
- Fox, J. L., J. F. Brannon, and H. S. Porter (1993), Upper limits to the nightside ionosphere of Mars, *Geophys. Res. Lett.*, *20*, 1339–1342.
- Green, A. E. S., and R. P. Singhal (1979), Microplume model of spatial yield spectra, *Geophys. Res. Lett.*, *6*, 625–629.
- Haider, S. A. (1999), Ionization and airglow in the Martian atmosphere, Technical Report, ISRO-PRL Tr-100-99, p. 1–67.
- Haider, S. A., S. P. Seth, E. Kallio, and K. I. Oyama (2002), Solar EUV and electron-proton-hydrogen atom produced ionosphere on Mars: Comparative studies of particle fluxes and ion production rates due to different processes, *Icarus*, *159*, 18–30.
- Haider, S. A., S. P. Seth, V. R. Choksi, and K. I. Oyama (2006), Model of photoelectron impact ionization within the high latitude ionosphere at Mars: Comparison of calculated and measured electron density, *Icarus*, *185*, 102–112.
- Hinson, D. P., R. A. Simpson, J. D. Twicken, G. L. Tyler, and F. M. Flassar (1999), Initial results from radio occultation measurements with Mars Global Surveyor, *J. Geophys. Res.*, *104*, 26,997–27,012.

- Jackman, C. H., R. H. Garvey, and A. E. S. Green (1977), Electron impact on atmospheric gases, 1, Updated cross sections, *J. Geophys. Res.*, **82**, 5092.
- Kliore, A. J., et al. (1965), Occultation experiment: Results of the first direct measurements of Mars atmosphere and ionosphere, *Science*, **149**, 1243–1248.
- Kliore, A. J., et al. (1972), The atmosphere of Mars from Mariner 9 radio occultation measurements, *Icarus*, **17**, 484–493.
- Kliore, A. J., et al. (1973), S band radio occultation measurements of the atmosphere and topography of Mars with Mariner 9: Extended mission coverage of polar and intermediate latitudes, *J. Geophys. Res.*, **78**, 4331–4351.
- Kolosov, M. A., V. M. Ivanov, D. S. Lukin, and Y. G. Spiridonov (1976), Radio occultation of the Martian ionosphere taking into account horizontal gradients of electron density, *Space Res.*, **16**, 1013–1017.
- Lopez-Valverde, M. A., D. P. Edwards, M. Lopez-Puertas, and C. Roldán (1998), Non local thermodynamic equilibrium in general circulation models of the Martian atmosphere, 1, Effects of the local thermodynamic equilibrium approximation on thermal cooling and solar heating, *J. Geophys. Res.*, **103**, 16,799–16,811.
- Martin, L. J. (1984), Clearing the Martian air: The troubled history of dust storm, *Icarus*, **57**, 317–321.
- Molina-Cuberos, G. J., H. Lichtenegger, K. Schwingenschuh, J. J. Lopez-Moreno, and R. Rodrigo (2002), Ion-neutral chemistry model of the lower ionosphere of Mars, *J. Geophys. Res.*, **107**(E5), 5027, doi:10.1029/2000JE001447.
- Mul, P. M., and J. W. McGowan (1979), Temperature dependence of dissociative recombination for atmospheric ions NO, O₂, N₂, *J. Phys. B*, **12**, 1591–1602.
- Nair, H., M. Allen, A. D. Anbar, Y. L. Yung, and R. T. Clancy (1994), A photochemical model of the Martian atmosphere, *Icarus*, **111**, 124–150.
- O'Brien, K., W. Friedberg, H. H. Sauer, and D. F. Smart (1996), Atmospheric cosmic rays and solar energetic particles at aircraft altitudes, *Environ. Int.*, **22**, (suppl. 1), S9–S44.
- Owen, T. S., K. Biemann, D. R. Rushneck, J. E. Biller, D. W. Homarh, and A. L. Lafleur (1977), The composition of the atmosphere and surface of Mars, *J. Geophys. Res.*, **82**, 4635–5410.
- Pesnell, W. D., and J. M. Grebowsky (2000), Meteoric Magnesium in the Martian atmosphere, *J. Geophys. Res.*, **105**, 1695–1703.
- Porter, H. S., and F. W. Jump Jr. (1978), Analytical total and angular elastic electron impact cross sections for planetary atmospheres, Tech. Rep. CSC/TM-78/CO17, prepared for NASA, Goddard Space Flight Centre, Comput. Sci. Corp., Greenbelt, Md.
- Rodrigo, R., E. Garcia-Alvarez, M. J. Lopez-Gonzalez, and J. J. Lopez-Moreno (1990), A non steady one dimensional theoretical model of Mars' neutral atmospheric composition between 30 and 200 km, *J. Geophys. Res.*, **95**, 14,975–14,810.
- Savich, N. A., and V. A. Samovol (1976), The night time ionosphere of Mars from Mars 4 and Mars 5 dual frequency radio occultation measurements, *Space Res.*, **XVI**, 1009–1010.
- Seth, S. P., S. A. Haider, and K. I. Oyama (2002), Photoelectron flux and nightglow emissions of 5577 and 6300 Å due to solar wind electron precipitation in Martian atmosphere, *J. Geophys. Res.*, **107**(A10), 1324, doi:10.1029/2001JA000261.
- Seth, S. P., U. B. Jayanthi, and S. A. Haider (2006a), Estimation of peak electron density in the upper ionosphere of Mars at high latitude (50°–70°N) using MGS ACC data, *Geophys. Res. Lett.*, **33**, L19204, doi:10.1029/2006GL027064.
- Seth, S. P., V. Brahmananda Rao, C. M. Esposito Santo, S. A. Haider, and V. R. Choksi (2006b), Zonal variations of peak ionization rates in upper atmosphere of Mars at high latitude using Mars Global Surveyor accelerometer data, *J. Geophys. Res.*, **111**, A09308, doi:10.1029/2006JA011753.
- Singhal, R. P., and A. E. S. Green (1981), Spatial aspects of low and medium energy electron degradation in atmospheric oxygen, *J. Geophys. Res.*, **85**, 4776–4785.
- Vasiliev, M. B., et al. (1975), Preliminary results of dual frequency radio occultation of the Martian ionosphere with the aid of Mars 5 spacecraft (in Russian), *KOsm. Issled.*, **13**, 48–51.
- Verigin, M. I., K. I. Gringauz, N. M. Shutte, S. A. Haider, K. Szego, P. Kiraly, A. F. Nagy, and T. I. Gombosi (1991), On the possible source of the ionization in the nighttime Martian ionosphere 1. Phobos 2 HARP electron spectrometer measurements, *J. Geophys. Res.*, **96**, 19,307–19,313.
- Vikas, S. (2004), Chemistry of the lower ionosphere of Mars, M.Tech Thesis, in Andhra Univ., India, p. 1–83.
- Zhang, M. H. G., J. G. Luhmann, and A. J. Kliore (1990), An observational study of the nightside ionosphere of Mars and Venus with radio occultation methods, *J. Geophys. Res.*, **95**, 17,095–17,107.

V. R. Choksi and S. A. Haider, Physical Research Laboratory, Ahmedabad, India. (haider@prl.res.in)

W. C. Maguire, NASA Goddard Space Flight Centre, Greenbelt, MA, USA.

V. Singh, Universita' degli Studi di Brescia, Italia.

M. I. Verigin, Space Research Institute, Moscow, Russia.